International Journal of Thermophysics, Vol. 22, No. 1, 2001

Viscosity and Surface Tension of Saturated Toluene from Surface Light Scattering (SLS)[1]

A. P. Fröba[2] and A. Leipertz[2, 3]

It is demonstrated that dynamic light scattering (DLS) on a horizontal gas–liquid interface can be used for the reliable determination of surface tension and liquid kinematic viscosity. In contrast to the more usual approaches of surface light scattering (SLS) spectroscopy, a setup is used and described here which makes it possible to measure the capillary wave propagation characteristics in the forward scattering direction at variable wave numbers. The experiments in this work rely on a heterodyne detection scheme and signal analysis by photon correlation spectroscopy (PCS). Surface tension and liquid viscosity data of the important and, thus, well-documented reference fluid toluene have been measured under saturation conditions over a wide temperature range, from 263 to 383 K. These data demonstrate the excellent performance of the surface light scattering technique. The achievable accuracy of this technique is discussed in detail for both properties in connection with reference values available in the literature.

KEY WORDS: dynamic light scattering; surface light scattering; surface tension; toluene; viscosity.

1. INTRODUCTION

Light scattering by thermally excited capillary waves on liquid surfaces or gas–liquid interfaces can be used for the investigation of viscoelastic properties of fluids. Based on early theoretical and experimental work [1–10], renewed interest in surface light scattering (SLS) in recent years has resulted in a number of new applications [11–20]. Objects of these investigations extend from simple fluids over polymer solutions, liquid crystals,

[1] Paper presented at the Fourteenth Symposium on Thermophysical Properties, June 25–30, 2000, Boulder, Colorado, U.S.A.

[2] Lehrstuhl für Technische Thermodynamik (LTT), Friedrich-Alexander-Universität Erlangen-Nürnberg, Am Weichselgarten 8, D-91058 Erlangen, Germany.

[3] To whom correspondence should be addressed.

0195-928X/01/0100-0041$19.50/0

surfactant monolayers, and supramolecular systems to high-temperature melts. The determination of the thermophysical properties, surface tension and viscosity, is of special interest for pure fluids and fluid mixtures. In this context the SLS method is well established for the investigation of the critical behavior of surface tension [5, 6, 8, 10], while, in general, for viscosity, due to instrumental broadening effects, a poor accuracy is reported in the literature. At the present time, application of the surface light scattering technique to simple fluid surfaces serves rather as a check of the somewhat complex calibration procedures involved with this technique [21].

In contrast, in the present work it is demonstrated that the SLS method can be used for a reliable determination of surface tension and viscosity–without any calibration procedure–with an accuracy comparable to or even better than that for conventional methods. After an introduction to the technique, the experimental setup is described, which allows the analysis of scattered light in the forward direction at relatively high and variable wave numbers of capillary waves. In the second part of the paper, the data evaluation procedure is introduced, and results for the surface tension and the liquid kinematic viscosity of toluene are discussed in comparison with literature. Data for this important reference fluid are obtained under saturation conditions and cover the temperature range from 263 to 383 K.

2. PRINCIPLE OF SURFACE LIGHT SCATTERING (SLS)

2.1. Surface Fluctuations

Liquid surfaces in macroscopic thermal equilibrium exhibit surface waves that are caused by the thermal motion of molecules and that are quantized in so-called "ripplons" [1]. Based on a classical hydrodynamic approach, thermally excited surface fluctuations result in typical amplitudes of about 10 nm and wavelengths of about 10 μm [2, 3]. In order to excite surface fluctuations, work has to be done against the forces acting on a liquid surface. Due to the typically small values of the wavelengths and amplitudes, capillary forces dominate, while gravitational forces can be neglected [10].

In general, for the temporal decay of surface fluctuations two cases may be distinguished. In the case of high viscosity and/or low surface tension, the amplitude of surface waves is damped exponentially, while in the case of low viscosity the amplitude decays in the form of a damped oscillation as it is relevant in this work. Therefore, in the following, an overdamped behavior of surface fluctuations is not discussed.

A thermally excited surface can be represented by a superposition of waves with different amplitudes ξ_q and wave vectors $\vec{q}$ [10]. For a particular surface mode with frequency α, the time-dependent vertical displacement ξ of the surface to its flat equilibrium state at a given point $\vec{r}$ is given by

$$\xi(\vec{r}, t) = \xi_q \exp[i(\vec{q}\vec{r} + \alpha t)] \tag{1}$$

For the propagation of capillary waves on a vapor–liquid interface, the complex frequency α of a certain surface mode can be represented in first-order approximation by

$$\alpha = \omega + i\Gamma \approx \left[\frac{\sigma q^3}{\rho' + \rho''}\right]^{1/2} + i2q^2 \frac{\eta' + \eta''}{\rho' + \rho''} \tag{2}$$

where σ is the surface tension, ρ' and ρ'' are the densities of the liquid and vapor phases, respectively, and η' and η'' are the dynamic viscosities of the liquid and vapor phases, respectively. Furthermore, the real part in Eq. (2) represents the frequency ω and the imaginary part the damping Γ of the surface mode. A more exact description of the dynamics of surface waves dependent on the surface tension, viscosity, and density of the liquid and vapor phases and the wave vector is obtainable by solving the dispersion equation,

$$\left[i\alpha + 2q^2 \frac{\eta' + \eta''}{\rho' + \rho''}\right]^2 + \frac{\sigma q^3}{\rho' + \rho''} - 4q^4 \left[\frac{\eta' + \eta''}{\rho' + \rho''}\right]^2 \left[1 + \frac{i\alpha}{q^2} \frac{\rho' + \rho''}{\eta' + \eta''}\right]^{1/2} = 0 \tag{3}$$

A more detailed and rigorous consideration of the dynamics of surface waves on liquid surfaces or gas–liquid interfaces can be found in the literature, see, e.g., Refs. 2, 4, 6, 7, and 21.

2.2. Scattering Geometry

Light interacting with a oscillating surface structure is scattered. The scattering geometry used in this work is shown in Fig. 1, where scattered light is observed in the forward direction near refraction. This arrangement has been chosen due to signal and stability considerations [22] and differs from the more commonly employed scattering geometry, where the scattered light is observed close to the direction of the reflected beam. By the choice of the angle of incidence ε, resulting in a specific angle δ of the refracted light, and the scattering angle Θ_s,the scattering vector $\vec{q} = \vec{k}'_I - \vec{k}'_S$ is determined and, by this, the wave vector and frequency of the observed surface vibration mode. Here, $\vec{k}'_I$ and $\vec{k}'_S$ denote the projections of the wave vectors of the refracted ($\vec{k}_I$) and scattered light ($\vec{k}_S$) in the surface plane,

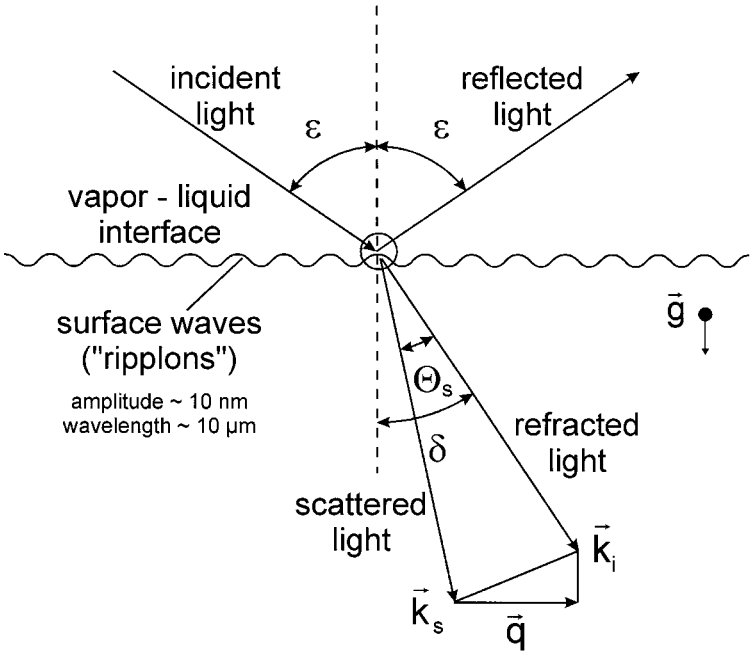

Fig. 1. Scattering geometry.

respectively. For the observation of scattered light within the irradiation plane and assuming elastic scattering (i.e., $k_I \cong k_S$), the modulus of the scattering vector is obtained as

$$q = |\vec{k}'_I - \vec{k}'_S| \cong 2k_I \sin(\Theta_S/2) \cos(\delta - \Theta_S/2)$$

$$= \frac{4\pi n}{\lambda_0} \sin(\Theta_S/2) \cos(\delta - \Theta_S/2) \tag{4}$$

where n is the fluid refractive index and λ_0 is the laser wavelength in vacuo.

2.3. Correlation Technique

In light scattering experiments the surface oscillations described result in a temporal modulation of the scattered light intensity, which contains information on the dynamics of the surface. Information about these processes can be derived by a temporal analysis of the scattered light using photon correlation spectroscopy (PCS). For heterodyne conditions, where the scattered light is superimposed with coherent reference light, e.g., with

stray light from the windows of the measuring cell, the time correlation function for the analysis of surface fluctuations is described by [21]

$$G^{(2)}(\tau) = A + B\cos(\omega\tau)\exp(-\tau/\tau_C) \tag{5}$$

where the correlation time τ_C and the frequency ω are identical to the time decay behavior ($\Gamma = 1/\tau_C$) and the frequency of the surface oscillations. A and B are experimental constants. The correlation function can thus be used for the evaluation of the desired properties, surface tension and viscosity; see Eq. (2) for a first-order approximation.

3. EXPERIMENTAL

The experimental setup is shown in Fig. 2. A frequency-doubled continuous-wave Nd : YVO_4-laser operated in a single mode with a wavelength of $\lambda_0 = 532$ nm serves as a light source. The laser power was about 250 mW when working at temperatures $T < 300$ K and somewhat lower for higher temperatures. For the observation of light scattered by surface waves, the optical path has to be aligned in a way that the laser beam and the direction of detection intersect on the liquid–vapor interface in the

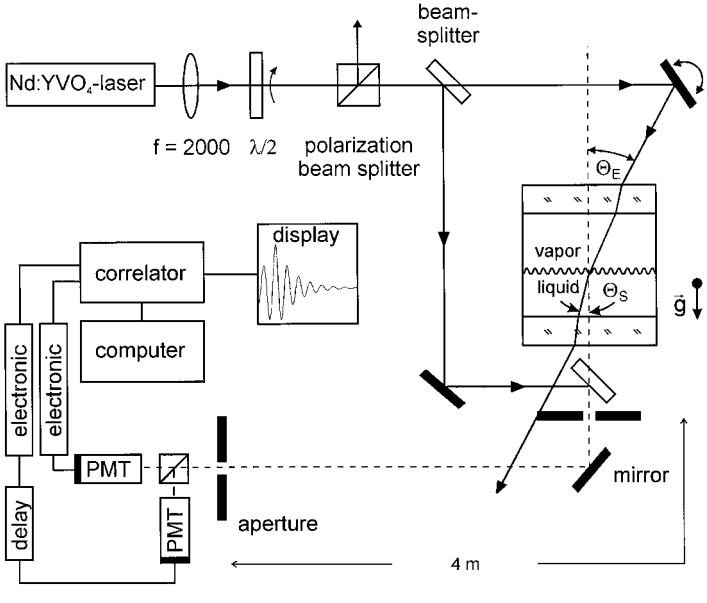

Fig. 2. Experimental setup: optical and electronic arrangement.

measurement cell. For large scattering intensities from the vapor–liquid interface, scattered reference light from the cell windows is not sufficient to realize heterodyne conditions. Here, an additional reference beam is added. To this end, part of the incident laser light is split by a glass plate and superimposed with the scattered light behind the sample cell. The time-dependent intensity of the scattered light is detected by two photomultiplier tubes (PMTs) operated in cross-correlation to suppress after-pulsing effects. The signals are amplified, discriminated, and fed to a digital correlator with 256 linearly spaced channels operated with a sample time down to 50 ns. Light scattered on the liquid–vapor interface is detected perpendicular to the surface plane, which means, $\Theta_S = \delta$ (see Fig. 1). For this arrangement, with the help of Snell's refraction law and simple trigonometric identities, the modulus of the scattering vector q can be deduced as a function of the easily accessible angle of incidence

$$q = \frac{2\pi}{\lambda_0} \sin(\Theta_E) \tag{6}$$

For the measurement of the angle of incidence Θ_E, the laser beam is first adjusted through the detection system consisting of two apertures ($\varnothing$, 1 to 2 mm) at a distance of about 4 m. Then the laser beam is set to the desired angle. For the experiment the angle of incidence Θ_E was set between 3.0 and 4.5° and was measured with a high precision rotation table. The error in the angle measurement has been determined to be approximately $\pm 0.005°$, which results in a maximum uncertainty of less than 1% for the desired thermophysical properties.

According to the specification of the manufacturer (Merck GmbH, Darmstadt), the toluene sample was of spectroscopic grade (Uvasol) with a minimum purity of 99.9% and was used without further purification. For the present measurements, the sample was filled from the liquid phase into an evacuated cylindrical pressure vessel (diameter, 70 mm; volume, 150 cm^3) equipped with two quartz windows (Herasil I; diameter, 30×30 mm). The temperature regulation of the cell surrounded by an insulating housing was realized with electrical heating. For temperatures below room temperature, the insulating housing was cooled to about 10 K below the desired temperature in the sample cell by a lab thermostat. The temperature of the cell was measured with two calibrated Pt 100-Ω resistance probes, integrated into the main body of the vessel, with a resolution of 0.25 mK using an AC bridge (Paar; MKT 100). The accuracy of the absolute temperature measurement was better than ± 0.015 K. The temperature stability during an experimental run was better than ± 0.001 K. For each temperature, at least six measurements at different angles of incidence were performed, where the

laser was irradiated from either side with respect to the axis of observation to check for a possible misalignment. The measurement times for a single run were typically of the order of 10 min down to a few seconds for the highest temperatures in this study.

4. MEASUREMENT EXAMPLE AND DATA EVALUATION

Figure 3 shows an example of a correlation function as obtained by scattering on a liquid–vapor interface of toluene under saturation conditions at a temperature of 303.15 K. The experimental correlation function, Eq. (5), has to be evaluated for the central quantities ω and τ_C, which may be done directly by a standard nonlinear fit in which the squared sum of residuals is to be minimized. Within the fit range of interest here, no systematic deviations can be observed. This is illustrated in the example of the residual plot in Fig. 3 and was confirmed for all measurements. The

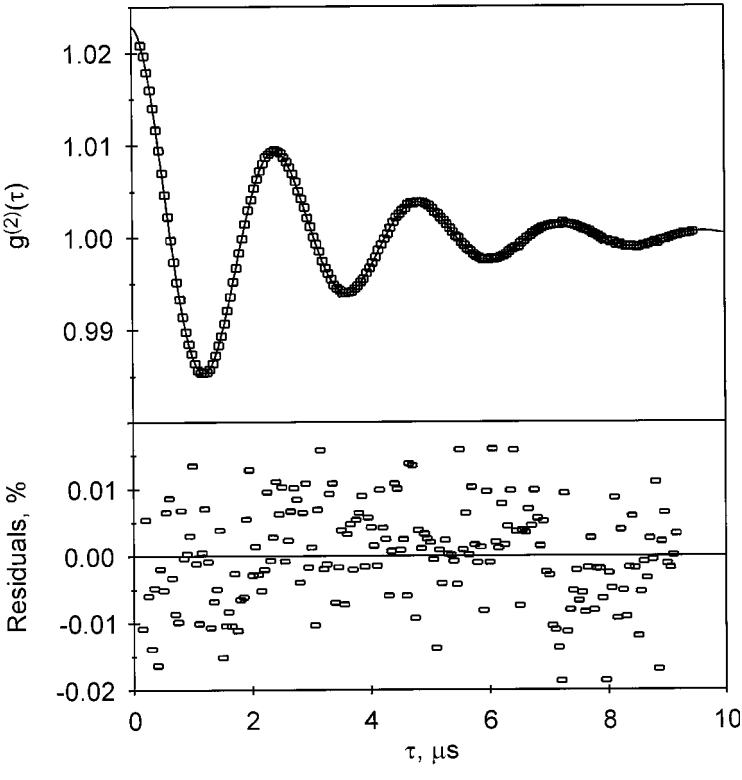

Fig. 3. Fit to a normalized experimental correlation function and residuals.

fit to the experimental correlation function results in a frequency of $\omega = 2.6035 \times 10^6\,\mathrm{rad \cdot s^{-1}} \pm 0.03\,\%$ and a decay time of $\tau_c = 2.701 \times 10^{-6}\,\mathrm{s} \pm 0.2\,\%$. The standard errors obtained from the fit may be compared with the deviations obtained from fits to various fit intervals, varying the first channel included in the fit in a range up to $0.5\tau_C$ and the last channel in a range starting at $2\tau_C$. With this procedure, the standard deviations of these individual fits are 0.04 % for ω and 0.3 % for τ_C. It should be noted here that either value is indicative only of the order of magnitude of the uncertainty that is related to the determination of the frequency and decay time of the measured correlation function. It is obvious that the error in the determination of the frequency is one order of magnitude smaller than that of the decay time.

The evaluation of the experimental data for the desired quantities viscosity and surface tension has always been performed on the basis of a full solution of the dispersion relation, Eq. (3). The necessity for this approach is illustrated in Fig. 4, where experimental values for the damping $\Gamma\,(=1/\tau_C)$ and frequency ω for a vapor–liquid interface of toluene at temperatures of 303.15 and 373.15 K are shown over a wide range of wave numbers. The solid and dashed lines indicate the theoretical variations obtained by an exact numerical solution of the dispersion equation [Eq. (3)] and by a derivation according to the first order approximation [Eq. (2)], respectively. For both calculations data for the density of the liquid and vapor phases have been adopted from the equation of state (EOS) of Goodwin [23]. Furthermore, the dynamic viscosity of the liquid phase was calculated from a correlation as given by Nieto de Castro and Vieira dos Santos [24], which is capable of describing most experimental data sets for toluene within their stated uncertainties, while data for the dynamic viscosity of the vapor phase are calculated theoretically according to a method given in Refs. 25 and 26. Finally, an estimation method for non-polar liquids as described in Ref. 26 was used to compute the surface tension of toluene. As can be seen from Fig. 4, with the exception of the highest wave numbers investigated in this work at a temperature of 303.15 K, where the scattered signal was weak and only a poor accuracy could be achieved, excellent agreement can be found for the measured values of ω and Γ with theoretical predictions based on an exact solution of the dispersion equation. In contrast to this, an increasing difference with increasing wave numbers is observable with respect to the first-order approximation. This behavior makes it clear, especially for the relatively high wave numbers studied in this work, that a reliable determination of surface tension and viscosity is possible only by an exact numerical solution of the dispersion equation, Eq. (3), where the frequency ω, the damping Γ, and the modulus of the scattering vector q are used as input values.

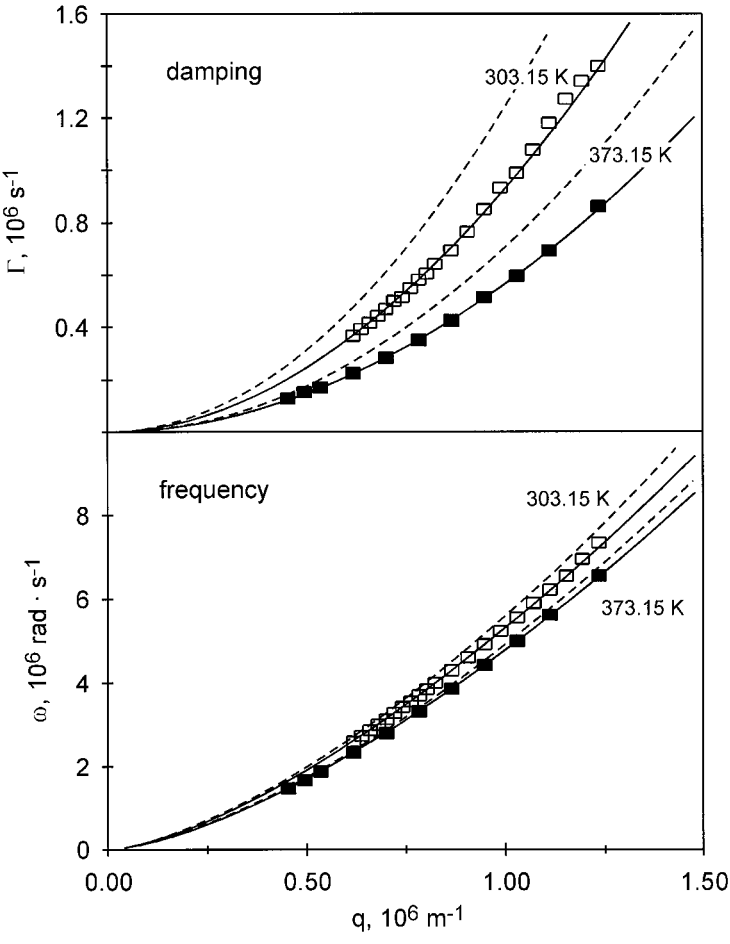

Fig. 4. Frequency ω and damping Γ of surface waves on a horizontal gas–liquid interface of toluene under saturation conditions depending on the wave vector q at a temperature of 303.15 and 373.15 K: (◪) experimental values from surface light scattering; (—) theoretically calculated values by a numerical solution of the dispersion equation, Eq. (3); (– –) theoretically calculated values by a first-order approximation, Eq. (2).

It should be emphasized that for the determination of surface tension and viscosity we always used wave numbers over a range from about 0.6 to $1.1 \times 10^6\ m^{-1}$. The lower limit was chosen so that instrumental broadening effects are negligible, while the limitation to q-values smaller than $1.1 \times 10^6\ m^{-1}$ is due to a weak scattering signal, as mentioned above.

5. EXPERIMENTAL RESULTS AND DATA CORRELATION

The quantity directly accessible in surface light scattering experiments is the ratio $\tilde{\sigma} = \sigma/(\rho' + \rho'')$ of the surface tension σ to the sum of the densities of the liquid and vapor phases. Similarly, also the direct quantity $\tilde{\nu}$ obtained for the viscosity is determined by both vapor and liquid properties, i.e., $\tilde{\nu} = (\eta' + \eta'')/(\rho' + \rho'')$, where η' and η'' are the dynamic viscosities of the liquid and vapor phases, respectively. If appropriate reference data for the quantities of the vapor phase are not available, the approximation $\tilde{\nu} \approx \nu'$ can be used, which relies on the neglect of vapor properties compared with the respective liquid quantities, and thus yields an approximate kinematic liquid viscosity. An estimation based on our experimental values for the quantity $\tilde{\nu}$, data for the liquid and vapor densities from the work of Goodwin [23], and theoretically calculated values for the dynamic viscosity of the vapor phase according to the method given in Refs. 25 and 26 indicates that for toluene the approximation would result in a systematic deviation from the exact kinematic viscosity value of about +1% for the lowest temperatures studied in this work (see Fig. 5). With increasing temperature the systematic error caused by neglecting the influence of the vapor phase would increase up to +3%. In the present work, however, data obtained for $\tilde{\nu}$ and $\tilde{\sigma}$ by an exact solution of the equation of dispersion

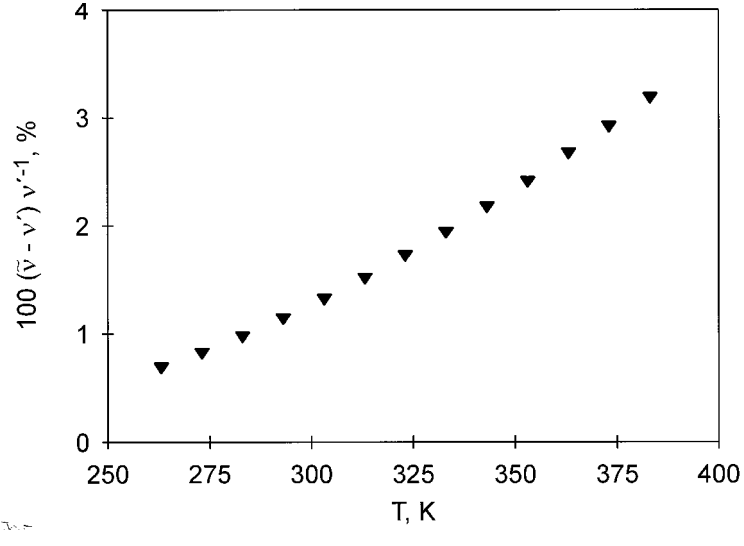

Fig. 5. Deviation between the direct accessible quantity $\tilde{\nu}$ for the viscosity from surface light scattering and the kinematic viscosity ν' of liquid toluene under saturation conditions.

for surface waves [see Eq. (3)] have been combined with theoretically calculated data for the dynamic viscosity of the vapor phase (see Refs. 25 and 26) and with density data for both phases from the EOS of Goodwin [23], to obtain results for the surface tension σ and liquid kinematic viscosity ν'.

The results for the desired quantities from surface light scattering are summarized in Table I. The listed data are average values of at least six independent measurements with different angles of incidence Θ_E. Also listed in Table I are the quantity $\tilde{\nu}$ obtained for the viscosity directly from the experiment and the values from the literature used for data evaluation as described above. With the approach given in Refs. 25 and 26, the vapor viscosity data can normally be predicted within $\pm 10\%$ for the temperature range studied in this work, which does not have any appreciable influence on the total uncertainty of better than 1% for the liquid kinematic viscosity. This estimate for the uncertainty of the viscosity values is obtained from

$$\Delta\nu' \approx \left[\left[\frac{\rho' + \rho''}{\rho'} S_{\tilde{\nu}} \right]^2 + \left[\frac{1}{\rho'} \Delta\eta'' \right]^2 + \left[\frac{\eta'' - \tilde{\nu}\rho''}{\rho'^2} \Delta\rho' \right]^2 + \left[\frac{\tilde{\nu}}{\rho'} \Delta\rho'' \right]^2 \right]^{1/2} \tag{7}$$

based both on the standard deviation $S_{\tilde{\nu}}$ of the measurement values and on the uncertainty of the reference data needed for the determination of the

Table I. Viscosity and Surface Tension of Toluene Under Saturation Conditions.[a]

T (K)	$\tilde{\nu}$ ($mm^2 \cdot s^{-1}$)	η'' ($\mu Pa \cdot s$)	ρ' ($kg \cdot m^{-3}$)	ρ'' ($kg \cdot m^{-3}$)	ν' ($mm^2 \cdot s^{-1}$)	σ ($mN \cdot m^{-1}$)
263.15	0.9965	6.06	892.3	0.02	0.9897	31.02
273.15	0.8710	6.29	883.7	0.04	0.8639	30.06
283.15	0.7707	6.52	874.9	0.07	0.7633	28.92
293.15	0.6870	6.76	866.1	0.11	0.6793	27.94
303.15	0.6180	6.99	857.1	0.18	0.6100	26.79
313.15	0.5606	7.23	848.0	0.28	0.5523	25.61
323.15	0.5104	7.46	838.8	0.42	0.5018	24.50
333.15	0.4710	7.71	829.5	0.62	0.4621	23.42
343.15	0.4343	7.96	820.0	0.89	0.4251	22.31
353.15	0.4052	8.21	810.3	1.24	0.3957	21.18
363.15	0.3766	8.47	800.5	1.70	0.3668	20.19
373.15	0.3543	8.74	790.4	2.27	0.3443	19.10
383.15	0.3332	9.01	780.2	2.99	0.3229	17.99

[a] T, temperature; $\tilde{\nu}$, quantity obtained for viscosity; η'', dynamic viscosity of the vapor phase; ρ', density of the liquid phase; ρ'', density of the vapor phase; ν', kinematic viscosity of the liquid phase; σ, surface tension.

true liquid kinematic viscosity from the direct observable $\tilde{\nu}$. In detail, for the relative uncertainty of the vapor viscosity $\Delta\eta''/\eta''$, liquid density $\Delta\rho'/\rho'$, and vapor density $\Delta\rho''/\rho''$, values of 10, 1, and 1%, respectively, have been estimated. As is true for many DLS applications [27], the standard deviation of individual measurements may be considered as a reasonable measure for the experimental uncertainty. In all instances, the value for $S_{\tilde{\nu}}$ was below 1%, which is determined mainly by the uncertainty of the angle measurement. The relative overall maximum uncertainty $\Delta\nu'/\nu'$ of our values for the liquid kinematic viscosity as estimated by Eq. (7) is displayed in Fig. 6. Here, the individual contributions of Eq. (7) related to $S_{\tilde{\nu}}$, $\Delta\eta''$, $\Delta\rho'$, and $\Delta\rho''$ are shown relative to the values of ν'. As can be seen from Fig. 6, for the whole temperature range studied in this work, the uncertainties in the used reference data have a comparatively small influence on the final results for liquid viscosities, so that for this quantity an overall maximum uncertainty of better than 1% could be established. In a similar way the uncertainty for the surface tension may be estimated. For the whole temperature range studied, the standard deviation $S_{\tilde{\sigma}}$ of individual measurements was in most cases below $\pm 0.5\%$, and although the accuracy of density data is of course far better than that of vapor viscosity data, some uncertainty is also introduced through the limited accuracy of the available density data. Yet in combination, a value of better than 1% may be regarded as a fair estimate for the total uncertainty of the surface tension.

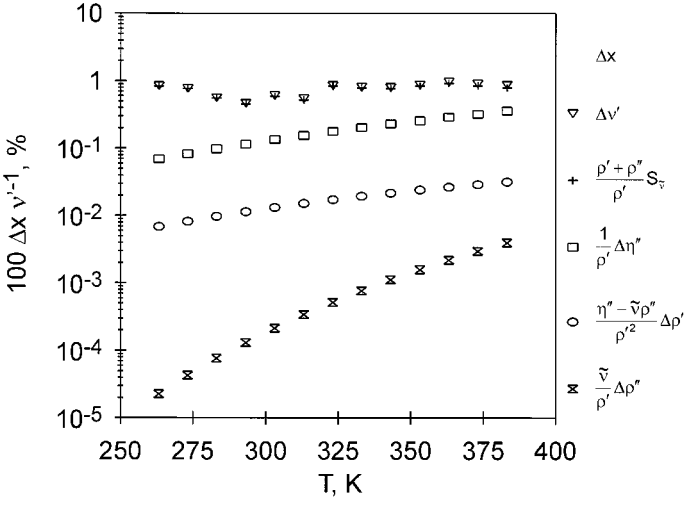

Fig. 6. Estimated overall maximum uncertainty for the liquid kinematic viscosity and individual contributions to that value.

Table II. Coefficients of Eq. (8)

ν'_0 ($mm^2 \cdot s^{-1}$)	0.013115
ν'_1 (K)	1057.46
ν'_2 (K^{-1})	0.0011597
rms (%)	0.14
T range (K)	263–383

For the whole temperature range studied in the present investigation, a modified Andrade-type equation, which in its simple form is commonly chosen to represent the dynamic viscosity at least over a limited temperature range, was used in the form

$$\nu' = \nu'_0 \exp[\nu'_1 T^{-1} + \nu'_2 T] \tag{8}$$

in order to represent our experimental kinematic viscosity data for toluene, where T is the temperature in kelvins and the coefficients are given in Table II. Here, also the standard deviation of our data relative to those calculated by Eq. (8) is listed. It should be noted that the residuals of the experimental data from the fit are smaller than the standard deviation of the individual measurements. The experimental data for the surface tension can be well represented by a linear equation of the form

$$\sigma = \sigma_0 + \sigma_1 T \tag{9}$$

where the fit parameters σ_0 and σ_1 are given in Table III. The present correlation represents the experimental values of the surface tension with a root-mean-square deviation of about 0.2%.

6. COMPARISON WITH LITERATURE DATA

In Fig. 7 our values for the kinematic viscosity of toluene under saturation are shown in comparison to available literature data from the last 20 years. Deviations between our results from surface light scattering and

Table III. Coefficients of Eq. (9)

σ_0 ($mN \cdot m^{-1}$)	59.933
σ_1 ($mN \cdot m^{-1} \cdot K^{-1}$)	−0.10952
rms (%)	0.21
T range (K)	263-383

the reference values are plotted using our correlation, Eq. (8), as a basis. Data for the viscosity included in Fig. 7 comprise measurements of Medani and Hasan [28] performed by a rolling ball viscometer, a method for which it is questionable if low uncertainties can be achieved, and data by Dymond and Robertson [29] obtained with a capillary viscometer with a stated uncertainty of $\pm 0.5\,\%$. The measurements by Byers and Williams [30], Gonçalves et al. [31], and Kaiser et al. [32] were performed by Ubbelohde capillary viscometers with claimed uncertainties of 0.3, 0.3, and around 1 %, respectively. These data sets and the compilation by Vargaftik [33] refer to atmospheric pressure; the deviation from saturation values is negligible for the whole temperature range in this study, where the maximum saturation pressure is 0.1 MPa. Finally, besides the already mentioned

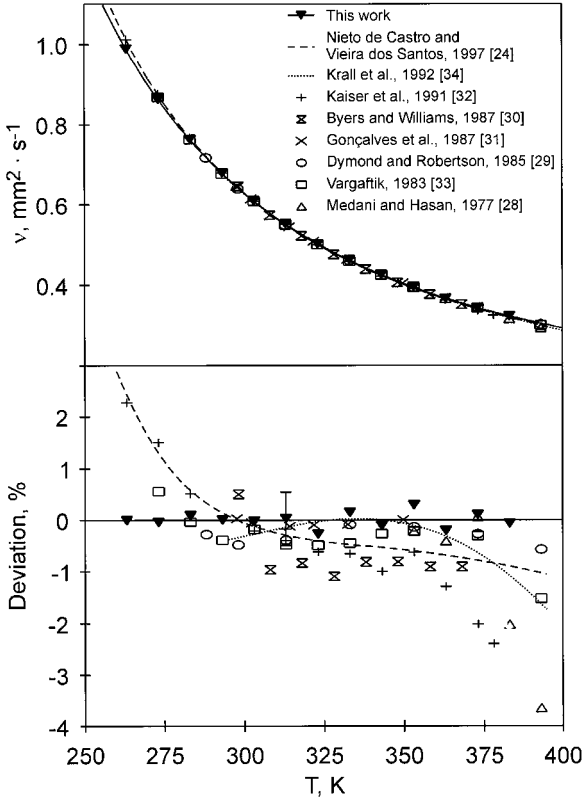

Fig. 7. Kinematic viscosity of liquid toluene under saturation conditions from surface light scattering in comparison to the literature.

correlation by Nieto de Castro and Vieira dos Santos [24], which describes the most recently reported experimental data sets within stated uncertainties, a correlation by Krall et al. [34] has been included, which is based on experimental values from an oscillating-disc viscometer with a stated experimental uncertainty of $\pm 0.5\%$. For computation using these correlations and conversion of the data in Refs. 28 and 33 from dynamic to kinematic viscosity, density data from the equation of state by Goodwin [23] have been employed. Figure 7 shows excellent agreement between our data from surface light scattering and those given by Gonçalves et al. [31] and by Dymond and Robertson [29]. Within the combined uncertainties this statement also holds for the data given by Dymond and Robertson [29] and for the correlation by Krall et al. [34]. Furthermore, particularly good agreement with an average deviation of 0.34% can be found between the fit of our data and the compilation by Vargaftik [33]. For the viscosity correlation given by Nieto de Castro and Vieira dos Santos [24] and the experimental data by Kaiser et al. [32] at low temperatures ($T < 275$ K), a positive deviation from our values is observed, which slightly exceeds the combined uncertainties. The fundamental similar behavior of both data sets at low temperatures may reflect that the correlation of Nieto de Castro and Vieira dos Santos [24] is based only on the experimental data of Kaiser et al. [32]. While for temperatures above 275 K, good agreement can be found between our values and the correlation given by Nieto de Castro and Vieira dos Santos [24]; for the data of Kaiser et al. [32], deviations from our data are observed that exceed the combined uncertainties. It should be noted, as our experimental values were limited to a maximum temperature of 383.15 K, the regression, Eq. (8), takes the character of an extrapolation at higher temperatures.

Values for the surface tension of toluene from surface light scattering are plotted in Fig. 8 together with available reference data extending over the past century. For data comparison only, references are taken into account which include at least three surface tension values at different temperatures. All experimental data displayed in Fig. 8 by symbols are based on the capillary rise method [35–41], with the exception of the data sets by Donaldson and Quayle [42] and Buehler et al. [43], which are determined by the maximum bubble pressure method. Furthermore, all experimental data refer to atmospheric pressure, with the exception of the data by Morino [36], which were obtained under saturation conditions. While in Fig. 8 the depicted correlation of Körösi and Kováts [44] is based on their own experimental values from the capillary rise method, the correlation given by Jasper [45] is based on the work of Donaldson and Quayle [42]. The surface tension correlation given by Bonnet and Pike [46] is based on 58 experimental data points collected from the literature. Finally,

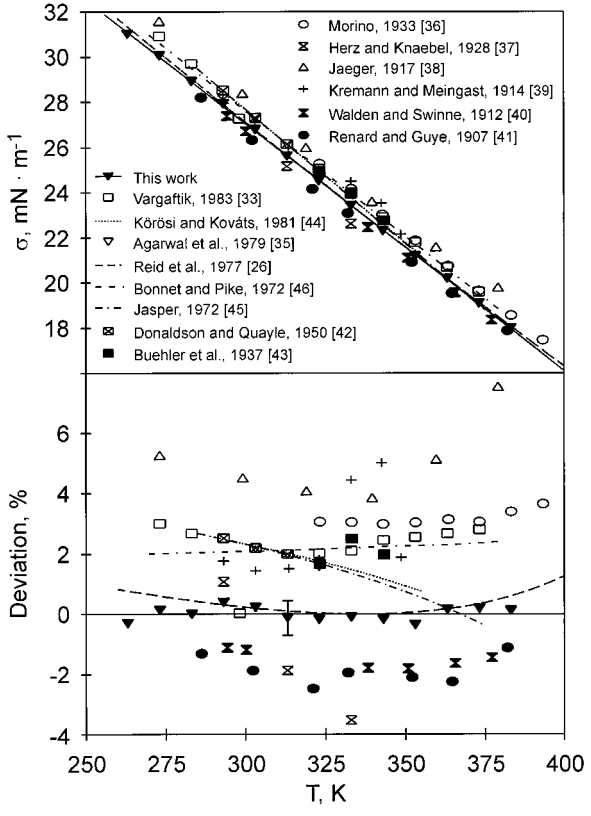

Fig. 8. Surface tension of toluene under saturation conditions from surface light scattering in comparison to the literature.

values from the data collection of Vargaftik [33] and an estimation by Reid et al. [26] as mentioned above are included in Fig. 8. Here, for the few data sets which explicitly give a statement for the uncertainty, a value between about 0.5 and 1% can be found. As can be seen from the deviation plot in Fig. 8, where the deviations between our results and the reference values are plotted using our correlation Eq. (9) as a basis, the maximum differences between the different data sets are slightly larger than 8%. The experimental data sets seem to form two bands, one clearly above and one clearly below our values from surface light scattering. In contrast to this behavior, for the whole temperature range investigated in the present study, good agreement between our values and the predictions of Reid et al. [26] can be found. Comparing our data with the recommended values

of Jasper [45], a decreasing deviation can be observed with increasing temperature. For these values the differences at low temperatures are outside the combined uncertainty, while good agreement can be found for temperatures $T > 330$ K. The same statement also holds for the work of Körösi and Kováts [44]. Summarizing, it seems that the surface tension of toluene is not known more accurately than $\pm 2\%$. It is not surprising that there are large discrepancies in the given values for surface tension, as the determination of this property may be affected by two factors which may not be easily controlled experimentally. First, values for surface tension are extremely susceptible to contamination. Second, if surface tension is measured for liquid–air systems, as in most cases cited above, the surface temperature may be somewhat below the temperature in the bulk of the fluid. An influence of this error, however, can be excluded for the present investigation, which has been carried out under saturation conditions in thermodynamic equilibrium.

7. CONCLUSIONS

Our investigations on a horizontal liquid–vapor interface of toluene under saturation conditions have shown that the surface light scattering technique can be utilized for an efficient and reliable determination of liquid kinematic viscosity and surface tension of transparent fluids. With the help of reference data for the liquid and vapor density and theoretically calculated data for the dynamic viscosity of the vapor phase—yet without any calibration procedure—an overall uncertainty of $\pm 1\%$ could be achieved for both properties of interest. Measurements have been performed over the temperature range from 263 to 383 K. For the kinematic viscosity the agreement with recent literature data can be regarded as satisfactory. For the surface tension of toluene a comparison of reference data covering the past century points to large differences, up to 8%, where our data from surface light scattering seem to form the center. With respect to recommended values for the surface tension of toluene, a maximum deviation of about -2.5% can be found for the lowest temperatures studied in this work. An improvement of the situation for the surface tension of toluene requires more accurate measurements under well-defined conditions.

ACKNOWLEDGMENTS

The authors would like to thank S. Will for many valuable discussions concerning the analysis and interpretation of the data. Parts of the work were supported by the Deutsche Forschungsgemeinschaft (DFG).

REFERENCES

1. W. Brouwer and R. K. Pathria, *Phys. Rev.* **163**:200 (1967).
2. R. H. Katyl and U. Ingard, *Phys. Rev. Lett.* **19**:64 (1967).
3. R. H. Katyl and U. Ingard, *Phys. Rev. Lett.* **20**:248 (1968).
4. E. H. Lucassen-Reynders and J. Lucassen, *Adv. Colloid Interface Sci.* **2**:331 (1969).
5. M. Giglio and G. B. Benedek, *Phys. Rev. Lett.* **23**:1145 (1969).
6. M. A. Bouchiat and J. Meunier, *Phys. Rev. Lett.* **23**:752 (1971).
7. M. A. Bouchiat and J. Meunier, *J. Physique* **32**:561 (1971).
8. J. Zollweg, G. Hawkins and G. B. Benedek, *Phys. Rev. Lett.* **27**:1185 (1971).
9. D. McQueen and I. Lundström, *J. Chem. Soc. Faraday Trans. I* **69**:694 (1973).
10. D. Langewin and J. Meunier, in *Photon Correlation Spectroscopy and Velocimetry*, NATO Advanced Study Institutes Series, Series B: Physics, Vol. 23, H. Z. Cummins and E. R. Pike, eds. (Plenum Press, New York, 1977), pp. 501–518.
11. A. Bttger and J. G. H. Joosten, *Europhys. Lett.* **4**:1297 (1987).
12. T. M. Jørgensen, *Meas. Sci. Technol.* **3**:588 (1992).
13. T. Nishio and Y. Nagasaka, *Int. J. Thermophys.* **16**:1087 (1995).
14. D. Sharpe and J. Eastoe, *Langmuir* **12**:2303 (1996).
15. A. P. Fröba, S. Will, and A. Leipertz, *Appl. Opt.* **36**:7615 (1997).
16. P. Tin, J. A. Mann, W. V. Meyer, and T. W. Taylor, *Appl. Opt.* **36**:7601 (1997).
17. D. Sharpe and J. C. Earnshaw, *J. Chem. Phys.* **107**:7493 (1997).
18. Q. R. Huang, C. H. Wang, and N. J. Deng, *J. Chem. Phys.* **108**:3827 (1998).
19. Q. R. Huang and C. H. Wang, *J. Chem. Phys.* **109**:6103 (1998).
20. D. M. A. Buzza, J. L. Jones, T. C. B. McLeish, and R. W. Richards, *J. Chem. Phys.* **109**:5008 (1998).
21. D. Langewin, *Light Scattering by Liquid Surfaces and Complementary Techniques* (Marcel Dekker, New York, 1992).
22. K. Sakai, P. K. Choi, H. Tanaka, and K. Takagi, *Rev. Sci. Instrum.* **62**:1192 (1991).
23. R. D. Goodwin, *J. Phys. Chem. Ref. Data* **18**, 1565 (1989).
24. C. A. Nieto de Castro and F. J. Vieira dos Santos, *personal communication* (Department of Chemistry and Biochemistry, University of Lisbon, Lisabon, 1997).
25. K. Lucas, *C. I. T.* **46**:157 (1974).
26. R. C. Reid, J. M. Prausnitz, and B. E. Poling, *The Properties of Gases and Liquids* (McGraw-Hill, New York, 1977 and 1987).
27. K. Kraft, M. Matos Lopes, and A. Leipertz, *Int. J. Thermophys.* **16**:423 (1995).
28. M. S. Medani and M. A. Hasan, *Can. J. Chem. Eng.* **55**: 203 (1977).
29. J. H. Dymond and J. Robertson, *Int. J. Thermophys.* **6**:21 (1985).
30. C. H. Byers and D. F. Williams, *J. Chem. Eng. Data* **32**: 344 (1987).
31. F. A. Gonçalves, K. Hamano, J. V. Sengers, and J. Kestin, *Int. J. Thermophys.* **8**:641 (1987).
32. B. Kaiser, A. Laesecke, and M. Stelbrink, *Int. J. Thermophys.* **12**:289 (1991).
33. N. B. Vargaftik, *Tables on the Thermophysical Properties of Liquids and Gases in Normal and Dissociated States* (Hemisphere, Washington, DC, 1983), pp. 347–348.
34. A. H. Krall, J. V. Sengers, and J. Kestin, *J. Chem. Eng. Data* **37**:349 (1992).
35. D. K. Agarwal, R. Gopal, and S. Agarwal, *J. Chem. Eng. Data* **24**:181 (1979).
36. Y. Morino, *Sci. Pap. Inst. Phys. Chem. Res. Jpn.* **23**:49 (1933).
37. W. Herz and E. Knaebel, *Z. Phys. Chem. Stoechiom. Verwandtschaftsl.* **131**:389 (1928).
38. F. M. Jaeger, *Z. Anorg. Allg. Chem.* **101**:1 (1917).
39. R. Kremann and R. Meingast, *Monatshefte Chem.* **35**:1332 (1914).
40. P. Walden and R. Swinne, *Z. Phys. Chem.* **79**:700 (1912).

41. T. Renard and P. A. Guye, *J. Chim. Phys.* **5**:81 (1907).
42. R. E. Donaldson and O. R. Quayle, *J. Am. Chem. Soc.* **72**:35 (1950).
43. C. A. Buehler, T. S. Gardner, and M. L. Clemens, *J. Org. Chem.* **2**:167 (1937).
44. G. Körösi and E. sz. Kováts, *J. Chem. Eng. Data* **26**:323 (1981).
45. J. J. Jasper, *J. Phys. Chem. Ref. Data* **1**:841 (1972).
46. J. C. Bonnet and F. P. Pike, *J. Chem. Eng. Data* **17**:145 (1972).